Chemical Engineering Science 261 (2022) 117993

Contents lists available at ScienceDirect

Chemical Engineering Science

journal homepage: www.elsevier.com/locate/ces

Upscaling microfluidic emulsification: the importance of sub-structure design in EDGE devices

Sten ten Klooster [a,*], Jelle van den Berg [a], Claire Berton-Carabin [a,b], Jolet de Ruiter [a], Karin Schroën [a]

[a] Laboratory of Food Process Engineering, Wageningen University, P.O. Box 17, Bornse Weilanden 9, 6708 WG Wageningen, the Netherlands
[b] INRAE, BIA, 44000 Nantes, France

HIGHLIGHTS

- Microfluidic emulsification is up-scaled using the so-called Multi EDGE design.
- This device has 75,000 droplet forming units producing 10 μm droplets at 0.3 m^3/m^2h.
- The flow resistance of dispersed phase supply channel determines productivity.
- Higher flow resistance leads to fast refilling of the 'pore' and droplet formation.

ARTICLE INFO

Article history:
Received 15 June 2022
Received in revised form 1 August 2022
Accepted 4 August 2022
Available online 8 August 2022

Keywords:
Microfluidic emulsification
Upscaling
Droplet formation
Monodisperse
Emulsion engineering
Interface

ABSTRACT

When used for emulsion production, microfluidics are known for their low energy usage and droplet monodispersity. However, current throughputs need to be improved to realize larger scale microfluidic emulsion production. Here, we present the upscaled device called Multi EDGE, which we use to produce 10-μm hexadecane droplets in 0.5 wt% SDS solution at 0.3 m^3/m^2h in a proof of concept study. The design of the dispersed phase supply channels is crucial, since a higher flow resistance causes a higher blow-up pressure and faster pore refilling. In turn, this results in high droplet formation frequencies of >1800 droplet s^{-1} per droplet formation unit, compared to maximally 60 droplet s^{-1} per droplet formation unit for devices with low-resistance substructure, which are limited by the refilling process. The fluxes and small droplets of Multi EDGE, show that these devices have potential for upscaling, especially when the substructure is designed properly.

1. Introduction

To produce emulsion products, such as mayonnaise, sunscreen and paint, the energy input may exceed the required energy input for creation of the interface by a factor 20 or more (Charcosset et al., 2004; Gijsbertsen-Abrahamse et al., 2004). Another disadvantage of conventional high-shear emulsification techniques is that they cause local fluctuations of energy density and cavitation, which makes it is hard to regulate the droplet sizes precisely. This leads to emulsions with wide droplet size distributions that are inherently less stable (Persson et al., 2014). Finally, these emulsification processes may lead to loss of protein functionality and the onset of lipid oxidation that influence chemical product stability in a negative way (Guo et al., 2020; Neves et al., 2017).

Compared to classic emulsification technologies, microfluidic emulsification is more subtle, and enables production of emulsions with a controlled droplet size, while preserving the nativity of the ingredients (Neves et al., 2017; Zhu and Wang, 2017). Microfluidic emulsification has been used for the interpretation of results in research areas such as biology, chemistry and particle synthesis, through the monodisperse droplets that are generated (Conchouso et al., 2014; Shen et al., 2016; Theberge et al., 2010).

Microfluidic emulsification starts by pushing the dispersed phase through a narrow channel until it reaches the continuous phase channel. Next, the dispersed phase adopts a droplet-like shape and snaps off, either spontaneously or due to the shear of the continuous phase flow. The microfluidic devices that operate by shear of the continuous phase flow (e.g., T- and Y-junctions, flow-focussing and co-flow devices) require very accurate flow control over the two phases, which is rather difficult, especially when multiple droplet formation units operate in close proximity (Vladisavljević et al., 2012; Zhu and Wang, 2017). In spontaneous

* Corresponding author.
E-mail address: sten.tenklooster@wur.nl (S. ten Klooster).

https://doi.org/10.1016/j.ces.2022.117993
0009-2509/

microfluidic emulsification techniques, snap-off occurs because of a difference in Laplace pressure, and only one phase has to be controlled precisely, which makes it more practical (Kawakatsu et al., 1997; Schroën et al., 2015).

Currently, microfluidic emulsification is applied at a small scale of maximally a few mL per hour for droplets with a size relevant to food production (<10 μm) (Schroën et al., 2015). For an industrial scale production of typically 20 m^3 per hour, many channels (in the order of billions) have to be operated in parallel, and therefore the major challenge for microfluidic emulsification is to scale up by numbering up (Gijsbertsen-Abrahamse et al., 2004; van Dijke et al., 2009; Vladisavljević et al., 2018;Schroën et al., 2015). A few successes have been reported in literature, such as: EDGE (Edge-based Droplet GEneration) (van Dijke et al., 2009, 2010c), (asymmetric) straight-through arrays (Kobayashi et al., 2009, 2008), Millipede (Amstad et al., 2016; Ofner et al., 2017), microchannels (Kobayashi et al., 2012; Vladisavljević et al., 2018), and STEP emulsification (Stolovicki et al., 2018). Not all these devices have shown the production of small droplets (±10 μm) that we target here.

Recently, we have introduced a novel microfluidic emulsification device called Partitioned EDGE (Sahin and Schroën, 2015), which is an improved version of regular EDGE, and explored its droplet formation mechanism (Deng et al., 2021; Ten Klooster et al., 2019). The productivity of these devices is determined by the fraction of active droplet formation units (DFUs), the droplet formation frequency per DFU, and the droplet size (larger droplets can be made at higher overall productivity (Stolovicki et al., 2018)). Besides, the surfactant as well as the viscosities of both phases affect the productivity (Sahin et al., 2016; van Dijke et al., 2010b; van Dijke et al., 2010a).

When upscaling microfluidic emulsification devices, it is desired to make the dispersed phase supply channels as short as possible to save space on the chip. Until now, the effect of sub-structure geometry on the production rates in spontaneous upscaled devices has never been considered to be relevant to the best of our knowledge. In this paper we present a device called Multi EDGE. It was manufactured with state-of-the-art cleanroom technologies, and it contains 75,000 DFUs. We report the performance of Multi EDGE for oil-in-water (O/W) emulsification and discuss its suitability for larger scale production. Here, we compare its productivity per DFU (DFU productivity) with the small scale Partitioned EDGE, which has 125 DFUs with the same DFU structure but a different sub-structure (Sahin and Schroën, 2015). This is done to explain how the sub-structure can be used to improve the productivity, therewith highlighting an aspect of microfluidics design that is generally not considered. Finally, we compare overall productivity (L/m^2h) between devices reported in literature, and we show that the productivity of Multi EDGE is relatively high compared to that of other devices from literature.

2. Materials and methods

2.1. Materials

Hexadecane (ReagentPlus® 99 %, Sigma-Aldrich, Germany) was used as the to-be-dispersed phase and 0.5 wt% sodium dodecyl sulphate (SDS, Merck, Germany) as the emulsifier. Ultrapure water (18.2 MΩ) was used for all experiments, and prepared using a Milli-Q system (Millipore Corporation, Billerica, MA, USA).

2.2. Microfluidic emulsification devices

In this research we used Multi EDGE, an upscaled microfluidic emulsification device and compared its productivity per DFU with Partitioned EDGE. Partitioned EDGE and Multi EDGE have several similarities: (1) the droplet formation unit consists of a 3D structure, with a pore ending in a deeper continuous phase channel where the droplets were formed, (2) the geometry of the DFUs has equal dimensions and (3) there is no cross-flow needed for droplet formation. The differences between the chips are in the amount of DFUs and the geometry of the sub-structures (Table 1), which is further explained below.

2.2.1. Partitioned EDGE

Partitioned EDGE has a shallow connection between the deeper continuous and dispersed phase channels (Fig. 1a,b) (Sahin and Schroën, 2015; Ten Klooster et al., 2019). The shallow connection consists of a main plateau and multiple micro-plateaus. The Partitioned EDGE has 25 micro-plateaus, which are the DFUs, with a length, width and height of 30, 10 and 2 μm respectively (Fig. 1 and Table 1). Fabrication of the Partitioned EDGE chips was done by Micronit Microfluidics, Enschede, The Netherlands and is explained in detail in a previous paper (Sahin and Schroën, 2015). The chip was placed in a chip holder from Micronit (Fluidic Connect PRO Chip Holder with 4515 Inserts, Micronit Microfluidics, Enschede, The Netherlands) and connected with standard tubing.

2.2.2. Multi EDGE

Silicon substrates of 400-μm thickness were used to fabricate the Multi EDGE chips (Fig. 1c,d). In the substrate, the micro- and the main plateaus were fabricated through deep reactive ion etching (Cytocentrics B.V., The Netherlands); the dimensions of the micro-plateaus (DFUs) were 10 × 2 μm (width × height). The Multi EDGE chip was placed in a custom-made module constructed by the technical workshop of Wageningen University. The Multi EDGE chip was 10 × 10 mm, and the part containing the DFUs was 5 × 6 mm, of which the effective pore area was 5 % (surface porosity based on DFUs). The overall, area-based productivity (in L/m^2h) was calculated based on the area that contained the DFUs (5 × 6 mm), as is commonly done in literature (e.g. (Kobayashi et al., 2005)). The main difference in device geometry between Multi EDGE and Partitioned EDGE was the height of the main plateaus (h) (Table 1). Technical limitations did not allow us to etch the main plateaus as shallow as the micro-plateaus (10 μm vs 2 μm). To research the effect of this change in substructure, we compared the droplet sizes and productivity per DFU with Partitioned EDGE that was described in section 2.3.1.

We did not observe monodisperse droplet formation with a Multi EDGE chip, which had dimensions of 5 × 2 μm (width × height) micro-plateaus. In other publications about STEP and microchannel emulsification, it was shown both experimentally and theoretically that the minimum aspect ratio of micro-plateaus (width / height, Fig. 1) has to be larger than ∼ 2.6 for

Table 1
Specifications of Partitioned EDGE and Multi EDGE devices.

EDGE Type	Micro-plateaus (DFUs)	Main plateaus			
	n_{mi} (per main plateau)	Dimensions $L \times W \times H$ [μm]	Spacing$S_1 \times S_2$ [μm]	n	Dimensions $l \times w \times h$ [μm]
Partitioned EDGE	25	30 × 10 × 2	10 × —	1	170 × 500 × 2
Multi EDGE	250	30 × 10 × 2	10 × 20	300	370 × 6000 × 10

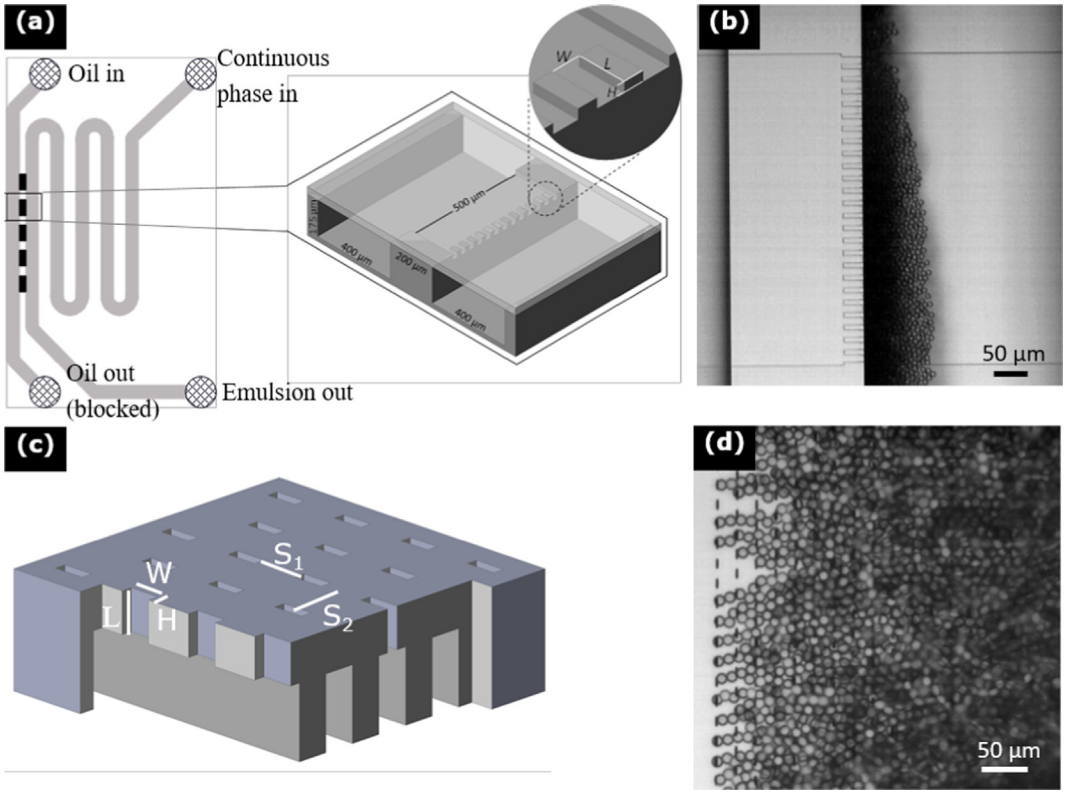

Fig. 1. (a) The Partitioned EDGE chip layout with five plateaus (black rectangles in left image), placed between the deep continuous and to-be-dispersed phase channels, and a close-up sketch of the micro-plateaus with their characteristic dimensions labelled in the middle circle (W = width, L = length and H = height). (b) Partitioned EDGE during emulsification. (c) Schematic 3D representation of Multi EDGE. (d) Multi EDGE during emulsification.

monodisperse droplet formation (Kobayashi et al., 2004; Montessori et al., 2019). Possibly this effect also plays a role in EDGE chips.

2.3. Cleaning of the devices

Both devices were thoroughly cleaned prior to operation to ensure their hydrophilicity and suitability for O/W emulsification (Van Dijke et al., 2008). Since the devices had a different configuration, they could not be cleaned in the same way. The Multi EDGE device was cleaned by flushing ethanol through the chip, and subsequently subjecting to plasma oxidation. The Partitioned EDGE device was cleaned by flushing ethanol through the chip and sonicating in ethanol. Next, It was baked in an ashing furnace (Carbolite AAF-1100, Carbolite Gero, Derbyshire, United Kingdom) at 500 °C for two hours.

2.4. Operation of the devices

Once cleaned, the devices could be used. First, the dispersed and continuous phases were prepared, using hexadecane and 0.5 wt% SDS in water, respectively. Next, each microfluidic chip was placed in its own holder. The continuous phase was then run through each chip to wet the device. After this, the oil was pushed in across the plateau, and the formed droplets were carried away by the cross-flowing continuous phase (Fig. 1bd). The cross-flow is oriented along the width of the DFUs in Partitioned EDGE and along the height of the DFU in Multi EDGE. The cross-flow is not needed for droplet formation, but only required to carry away the formed droplets that otherwise obscure observation. The flows were controlled through a microfluidic control system (Elveflow®, France), and droplet formation was monitored by using an inverted microscope (Axiovert 200 MAT, Carl Zeiss B.V., The Netherlands) connected to a high-speed camera (MotionPro HS-4, IDT Inc., USA) (maximum frame rate used for recording was 5000 Hz, maximum precision was 7.8 pixels μm^{-1}). High resolution videos were made with a high-speed camera (FASTCAM SA-Z, Photron Limited, Japan) at a frame rate of 100,000 frames per second and with a resolution of 0.973 µm/pixel to measure the time needed for droplet formation. Please note: for Multi EDGE we used top-view recordings (Fig. 1d), since we cannot look through the (silicon) channels.

2.5. Measuring droplet sizes

For both chips, 20–50 droplets per droplet size data point were analysed by image analysis software to determine the average droplet size and size distribution, as was done previously (Sahin and Schroën, 2015; Ten Klooster et al., 2019). Given the monodispersity of the droplets, this is an appropriate measurement method. This method has been compared to static light scattering previously and good agreement was found (van Dijke et al., 2010d). The size distribution of the droplets was expressed in the form of coefficient of variation, CV, which was defined as:

$$CV = \frac{\sigma}{d_{dr}} x\,100 \quad (1)$$

where σ is the standard deviation of the droplet diameters and d_{dr} is the number-average droplet diameter. Droplets with a CV below 10 % were considered monodisperse, which is based on previous research (Sahin et al., 2016; van Dijke et al., 2009).

2.6. Measuring down time and necking time

High resolution images at a maximum frame rate of 100,000 frames s^{-1} were used to determine the down time (DFU filling)

and necking time (actual droplet formation). The number of frames between the start of dispersed phase leaping into the deeper continuous phase channel and breakage of the neck was divided by the frame rate to obtain the necking time. The down time was determined in a similar way, starting with the neck breakage, and finishing with the dispersed phase leaping into the continuous phase channel again. This was done for several locations over the chip and for three droplets per DFU.

2.7. Flow resistance calculation

To compare various designs, the flow resistances are calculated. The flow resistance (R) of a rectangular channel can be calculated with a Hagen-Poiseuille equation:

$$R = \frac{12\eta_d l}{1 - 0.63(\frac{h}{w})} \frac{1}{h^3 w} \quad (2)$$

where η_d is the dispersed phase viscosity, l the length, h the height and w the width of the channel. Equation (2) was used to calculate the flow resistance of a micro-plateau and main plateau separately. The flow resistance of the main and micro-plateaus together (R_t) was defined as:

$$R_t = \frac{R_{mi}}{n_{mi}} + R_{ma} \quad (3)$$

where R_{mi} is the flow resistance of the micro-plateau, n_{mi} is the number of micro-plateaus per main plateau and R_{ma} is the flow resistance of the main plateaus. The flow resistance of the whole shallow connection, expressed per micro-plateau ($R_{t,mi}$) was calculated as:

$$R_{t,mi} = R_t \cdot n_{mi} \quad (4)$$

3. Results and discussion

We compared the droplet sizes and maximum productivity of the upscaled Multi EDGE (Fig. 1cd) with the small scale Partitioned EDGE (Fig. 1ab). The productivity of Multi EDGE was expressed per DFU (DFU productivity) to compare with Partitioned EDGE and per area (overall productivity) to compare with devices from literature.

3.1. Emulsion production with Multi EDGE

In this section we first describe the results for Multi EDGE (10 × 2 μm micro-plateaus); monodisperse hexadecane droplets were successfully produced over 8 h, which was the maximum time that we attempted due to lab closing hours. Also a recent publication by Vladisavljević et al. showed that long-term stable production of dichloromethane droplets (25 μm) with silicon microchannel (STEP) emulsification devices was possible (Vladisavljević et al., 2018). Droplet formation in Multi EDGE started at 95 mbar, and the droplet size remained constant at 11.0 μm and monodisperse up to 130 mbar with a CV of < 10 % (Fig. 2a, insert). Above 130 mbar, a few DFUs started to produce polydisperse droplets that are roughly-one order of magnitude larger in diameter, whereas the majority of DFUs still formed small monodisperse droplets. With increasing pressure, more DFUs show

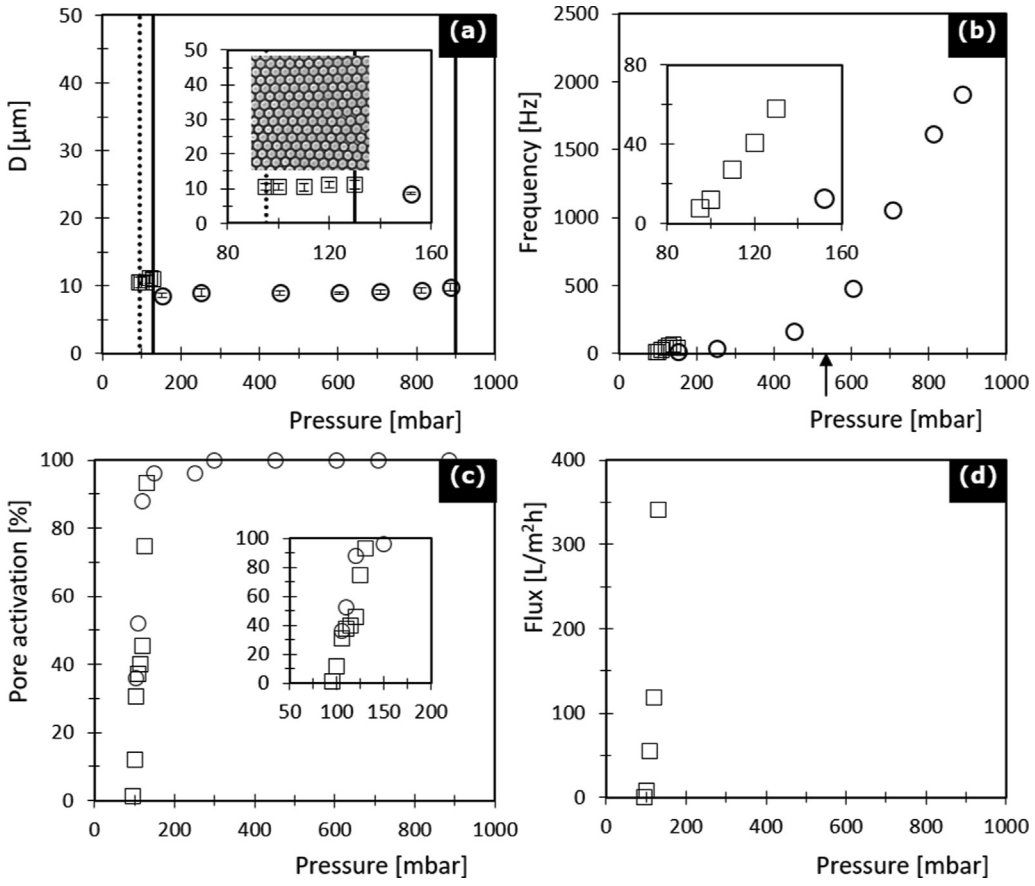

Fig. 2. Effect of dispersed phase pressure on: droplet size (a), droplet formation frequency (b), pore activation (c), and hexadecane flux (d) for Partitioned EDGE (○) and Multi EDGE (□). The dashed vertical lines denote the breakthrough pressure, the solid lines the blow-up pressures. The arrow in (b) indicates the LaPlace pressure of the meniscus when no surfactant is adsorbed. Error bars in (a) denote standard deviations.

this so-called blow-up behaviour, indicated by the vertical solid line (Fig. 2a). Both droplet formation frequency per DFU (Fig. 2b) and the number of active micro-plateaus (Fig. 2c) increased linearly with pressure, up to the point at which blow-up started occurring. Thus, the flux per area increased quadratically with pressure, till it reached blow-up (Fig. 2d). At this pressure (130 mbar), 93 % of the micro-plateaus were active with an average frequency of 58 Hz per micro-plateau, amounting to 313 L of oil per m^2h (assuming uniform performance over the entire surface of the device). This value is similar to values reported for STEP devices, where 91 % of the channels were active during production of 25-μm droplets (Vladisavljević et al., 2018). Multi EDGE will be further compared to other devices reported in literature in section 3.3.

3.2. Comparison of multi EDGE with partitioned EDGE

Both devices showed a start of droplet formation at a dispersed phase pressure of 95 mbar (dashed vertical line Fig. 2a), which therefore does not seem to be substantially influenced by the sub-structure design (more specifically, the main plateau height). For Partitioned EDGE, insufficient droplets were formed to measure the droplet size accurately, and therefore there is no data point at 95 mbar for Partitioned EDGE (Fig. 2a). This so-called breakthrough pressure is determined by the Laplace pressure, $P_{LP} = \gamma\,(1/R_1 + 1/R_2)\cos(\theta)$ of the meniscus (with radii R_1 and R_2) inside the micro-plateau working in the direction opposite to the applied pressure (P_{app}). Since the breakthrough pressure, the width, and height of the micro-plateaus (and thus R_1 and R_2) were constant, the devices should have a similar contact angle (θ). A contact angle increase of 10° may decrease the breakthrough pressure by ~ 5 mbar. The contact angle also influences the productivity (Maan et al., 2013), since it can reduce the blow-up pressure (Van Dijke et al., 2008), and thus decrease maximum productivity even by a factor two (Eggersdorfer et al., 2018). The low breakthrough pressure of 95 mbar indicates that – at least at low pressures – SDS adsorbed to the hexadecane-water meniscus, and thereby γ may reach as low as 8 mN/m (equilibrium value) compared to $\gamma \approx 44$ mN/m for an interface free of surfactant (Muijlwijk et al., 2016). When using the same components and concentrations in a Y-junction, it has been shown that the equilibrium interfacial tension was reached after ± 0.01 s, and a first reduction in interfacial tension was observed after < 0.001 s (Muijlwijk et al., 2016). This implies that the reduction in interfacial tension can be much faster than the droplet formation time at low droplet formation rates (<10 s^{-1}), although it may not be fast enough at high droplet formation rates (>1000 s^{-1}) (Ten Klooster et al., 2019).

The droplet sizes produced by Multi EDGE and Partitioned EDGE at the blow-up pressure were 11.0 and 9.8 μm, respectively. Droplet sizes have been shown to depend on DFU height (van Dijke et al., 2010b), which we kept as constant as possible at 2 μm for both devices. The droplets were indeed rather similar in size; slight differences may have occurred due to slightly different dimensions of the DFUs. DFU activation increased with pressure for both Multi EDGE and Partitioned EDGE, but did not seem to be influenced by main plateau height (Fig. 2c). As explained earlier, the DFUs start to become active when P_{app} exceeds P_{LP}, and since the DFUs have equal dimensions, our hypothesis was that all pores become active at this breakthrough pressure of 95 mbar. In reality, about three times the breakthrough pressure was required for an activity of 100 % (Fig. 2c). Similar effects were described by Abrahamse and coworkers for cross-flow membrane emulsification; as soon as the dispersed phase flows through one DFU, this prevents the neighbour DFUs from becoming active (Abrahamse et al., 2002).

When increasing the pressure beyond the breakthrough pressure for Multi EDGE, the droplet formation frequency per DFU initially increased faster compared to Partitioned EDGE (initial slopes in Fig. 2b), which is caused by the lower flow resistance of the main plateau in Multi EDGE. Just before blow-up, the maximum droplet formation frequency per DFU was ~ 30 times higher for Partitioned EDGE (blow-up pressure of 900 mbar) compared with Multi EDGE (blow-up pressure of 130 mbar). When including the slight difference in droplet size, the DFU productivity of hexadecane droplets by Partitioned EDGE was ~ 22 times higher.

To further improve the performance of microfluidic emulsification devices, we next identify the cause of the lower DFU productivity and blow-up pressure of Multi EDGE. To do so, we divide droplet formation into two stages: (1) necking and (2) down time. During necking, the dispersed phase leaps into the deeper continuous phase channel, where it adopts a droplet-like shape, which is still connected to the fluid on the plateau via a 'neck'. When the neck collapses (due to interfacial tension forces), the droplet is detached and with that the necking stage is finished (Fig. 3abc). Modelling studies have been performed leading to identification of local flow profiles (Montessori et al., 2019, 2018; van Dijke

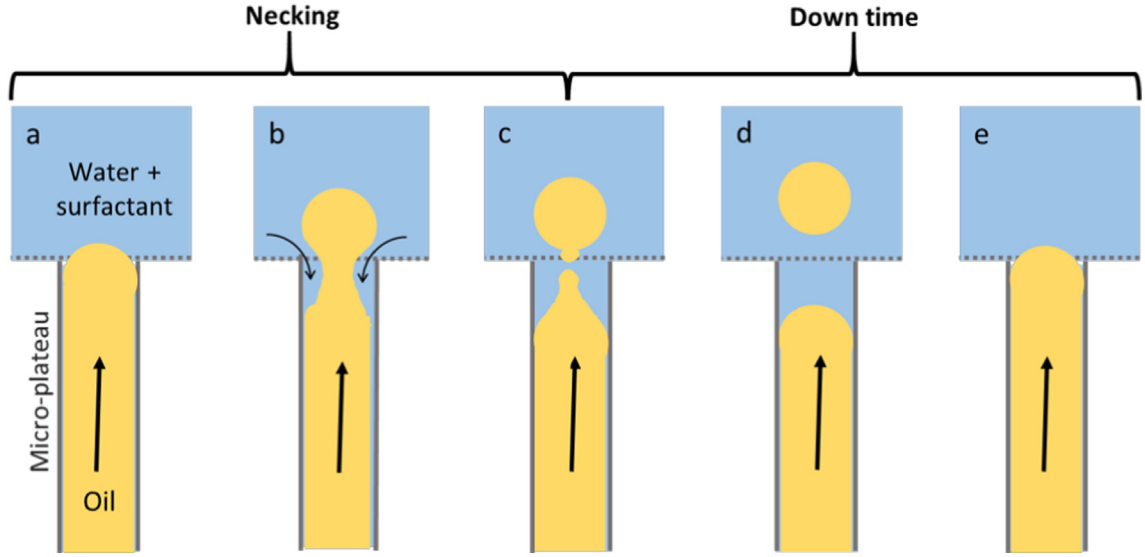

Fig. 3. The two stages of droplet formation; a-*b*-c depict necking and c-d-e depict down time.

Table 2
The droplet formation time, necking time, down time and the ratio between the down and necking time at the maximum productivity before blow-up, with standard deviations for Partitioned EDGE and Multi EDGE.

Chip	Drop formation time (ms)	Necking time (ms)	Down time (ms)	Ratio down / necking time
Multi EDGE	17 ± 2.1	1.5 ± 0.30	16 ± 2.1	10 ± 2.5
Partitioned EDGE	0.52 ± 0.021	0.33 ± 0.065	0.19 ± 0.069	0.59 ± 0.23

et al., 2010b). During the down time, the meniscus first retreats into the micro-plateau, after which the DFU refills (Fig. 3c,d,e). The latter only occurs when there is a positive pressure difference, which is defined as:

$$\Delta P_p = P_{app} - P_{LP} \tag{5}$$

So, to obtain a short down time (which is desired because this will increase the productivity), ΔP_p needs to be high, which is the case when P_{app} is high and/or P_{LP} is low; the first factor is determined by the blow-up pressure, and the latter is determined by the extent of surfactant adsorption at the interface. The down time ends when the dispersed phase leaps into the continuous phase channel again (Fig. 3e).

We measured necking and down times for both Multi EDGE and Partitioned EDGE at the highest pressures before blow-up P_{blowup} (Table 2). These results show that at high dispersed phase pressures, the down time is a substantial part of droplet formation for Multi EDGE. At lower pressures, the ratio of down/necking time would have been even higher because surfactant adsorption would be required to initiate refilling of the DFU (Deng et al., 2021). We found a down time of 16 ms for Multi EDGE versus 0.2 ms for Partitioned EDGE at P_{blowup}, which was the main cause for differences in productivity. The necking times were more comparable, although partitioned EDGE is still considerably faster as Multi EDGE (Table 2). So, ΔP_p will be higher in Partitioned EDGE than in Multi EDGE, which indicates that for Partitioned EDGE P_{app} is relatively high, and/or P_{LP} is relatively low.

We can calculate the average P_{LP} over the total droplet formation (necking + down time) from:

$$P_{LP} = P_{app} - \phi_{tot} \cdot R_{t,mi} \tag{6}$$

ϕ_{tot} (DFU flow rate) was calculated by multiplying the DFU frequency with the droplet volume; for $R_{t,mi}$ (the flow resistance of the whole shallow connection per micro-plateau, Equation (4)) and P_{app} we used values from Table 3. This results in an average P_{LP} of 122 mbar for Multi EDGE and 330 mbar for Partitioned EDGE. For both devices this is higher than the breakthrough pressure of 95 mbar, which indicates that the interfacial tension during down time is highly dynamic: just after droplet formation (Fig. 3c) barely any SDS has adsorbed yet, but over time SDS adsorption will occur (provided that the down time is long enough as would be the case in Multi EDGE), and the interfacial tension will gradually decrease (Fig. 3c-3e). When the applied pressure is higher than the P_{LP} of a *bare* hexadecane-water interface, the meniscus barely moves backwards after droplet formation (Fig. 3c) and immediately starts moving forward (Fig. 3d-e). This phenomenon was also used to explain the sudden exponential increase in bubble formation frequency when the applied pressure was higher than the P_{LP} of a *bare* air–water interface (Deng et al., 2021). In line with those results, we observed an increased productivity around an applied pressure of 530 mbar (Fig. 2b; arrow), which corresponds to the P_{LP} of a *bare* hexadecane-water meniscus ($P_{LP,\max}$) (Fig. 3d).

Table 3
The total flow resistance for one micro-plateau, the blow-up pressures and the Laplace counter pressures (as calculated by Eq. (6)) with standard deviations for Partitioned EDGE and Multi EDGE.

EDGE type	$R_{t,mi}$ (Pa s/m^3)	P_{app} (mbar)	P_{LP} (mbar) (mbar)
Partitioned EDGE	6.2E + 16	900 ± 20	122
Multi EDGE	1.9E + 16	130 ± 10	330

In contrast, for applied pressures below the Laplace pressure of a *bare* hexadecane-water interface, the meniscus will even momentarily move backwards, and droplet formation can only start if the Laplace pressure is lowered through SDS adsorption (Fig. 3cd). The subsequent forward motion is slow when the pressure difference is small resulting in a long down time. With Equation (6) we calculated an average P_{LP} for droplet formation, but we expect the P_{LP} during down time to be even higher than that because during the necking stage there is not an effective P_{LP} (Appendix). We expect that the average P_{LP} of the meniscus (Fig. 3d) for Partitioned EDGE during down time is close to that of a bare hexadecane-water interface ($P_{LP,\max}$ of 530 mbar). This also implies that the time-average ΔP_p for Multi EDGE in the situation shown in Fig. 3de is probably only a few mbar. For Partitioned EDGE this was probably a few hundred mbar, which means that the relative difference in ΔP_p between the devices was in the order of a factor of 100. The forward motion of the menisci (Fig. 3de) is determined by the pressure difference divided by the flow resistance of the device (Equation (6)). Since Multi EDGE has a 3.3 times lower $R_{t,mi}$ (Equation (6), Table 3), the actual difference in forward motion of the menisci between the devices would be in the order of 100/3.3, when operated at their maximum productivity. To summarize, the low flow resistance of Multi EDGE caused that at low pressures the viscous force already exceeds the interfacial tension force, resulting in a low blow-up pressure. The low blow-up pressure leads to a low ΔP_p, and therefore a long down time, leading to a low droplet formation frequency.

As mentioned, there was a factor 5 difference in necking time between Multi EDGE and Partitioned EDGE (Table 2). It was previously shown for bubbles that the necking time decreases with increasing applied pressure (Deng et al., 2021). We estimated the blow-up pressure of Multi EDGE with the Hagen-Poiseuille equation, based on the flow during necking of Partitioned EDGE. The values we calculate for Multi EDGE are high (270 mbar) compared to what we measured (130 mbar) (Appendix). The calculated value is still lower than $P_{LP,\max}$ (530 mbar), and therefore ΔP_p during down time would still be relatively low. This would result in a long down time, which would reduce the DFU productivity of Multi EDGE, again stressing the importance of the flow resistance of the sub-structure. The difference between the calculated blow-up pressure and measured blow-up pressure of Multi EDGE may be due to a difference in contact angle between the devices; in literature it has been suggested that an increase of 10° in contact angle can lead to a factor 2 difference in maximum productivity (Eggersdorfer et al., 2018). In addition, the difference in height between main and micro-plateau for Multi EDGE may have influenced the flow profile of the dispersed phase inside the micro-plateau and affect the instability needed for droplet formation (Fig. 3bc). For microchannels with diameters of a few hundred μm operated at low Reynolds numbers (<1) the entrance length is close to the hydraulic diameter. If we translate this directly through to our channels, this would imply an entrance length of around 3 μm (Galvis et al., 2012), which could be relevant given the device dimensions. To elucidate this, the sub-structure geome-

try should be systematically varied, which is part of follow up research.

A special feature in partitioned EDGE is that far beyond the blow-up pressure, large droplets are formed by the physical force that neighbouring droplets exert on each other by direct contact, and as this happens in a cascade fashion, this leads to a monodisperse emulsion (Ten Klooster et al., 2019). This was not observed for Multi EDGE, and most probably this has to do with the fact that in Multi EDGE the droplet formation units are positioned further apart, and the forming droplets are less confined as in Partitioned EDGE. Furthermore, at blow-up, slightly less droplet formation units are active, therewith increasing the average distance, and reducing the chance of interaction (Fig. 1).

3.3. Comparing Multi EDGE with other devices

Compared to Multi EDGE, straight-through microchannels (MCs) are the most similar upscaled microfluidic emulsification devices (Fig. 4). MCs receive the to be disperse phase by individual narrow channels that are all connected to the same general feeding area (Fig. 4a), whereas EDGE devices receive the to be dispersed phase from a common (main) plateau (Fig. 4b). These differences in device geometry are thought to influence DFU activity. For asymmetric straight-through MCs the fraction of active channels increases with oil viscosity. For instance, 50 % and 95 % of the channels were active for the preparation of ~ 30 μm tetradecane (viscosity of ~ 3 mPa s) and soybean oil droplets (typical viscosity of 50–60 mPa s), respectively (Vladisavljević et al., 2011). According to the reasoning that we used before for EGDE devices (equation (5)), the high viscosity oil will flow more slowly, which increases the chances for activation of neighbouring DFUs (Abrahamse et al., 2002). In line with this, the DFU activation of symmetric straight-through MCs decreased to 12 % when making smaller (9.8 μm) soybean oil droplets, which is probably caused by the higher applied pressures needed to overcome the Laplace pressure of the meniscus in this narrower channel (Fig. 3d) (Kobayashi et al., 2008). In EDGE devices early blow-up is prevented by the flow resistance of the substructure, which increases pore activation (Fig. 2c). This is an important lead for microfluidic design (e.g. making longer DFUs).

For small droplet (~10 μm) production, Multi EDGE devices seem to hold a competitive advantage due to their high microplateau activation (93 %). Ideally, we would like to compare the throughput of EDGE and MCs for similar droplet sizes and oil viscosities, but we could not find this combination in literature. However, a derived comparison is possible. In MCs studies a throughput of 2700 L/m^{2}h was found for 30-μm tetradecane droplets, and it was suggested that the throughput would be an order of magnitude lower when 10-μm droplets are targeted (Vladisavljević et al., 2011). Therefore we like to think that the current Multi EDGE design, with its 313 L/m^{2}h throughput for 10-μm hexadecane droplets, performs similarly to straight-through MCs.

We have also shown that there is still considerable room for improvement for Multi EDGE, and this may also be the case for straight-through MCs. As discussed earlier, if the frequencies obtained with partitioned EDGE can be reached in Multi EDGE by increasing the flow resistance of the device, this would imply approximately a 20-fold higher DFU productivity. In addition, when using hexadecane as the dispersed phase in a regular EDGE device, productivity increased by a factor 40 when using 5 wt% of α-lactalbumin (a dairy protein) as an emulsifier instead of 0.5 wt% of SDS (Sahin et al., 2016). These effects clearly indicate that much higher productivity is feasible when product formulation is used as an additional variable.

3.4. Outlook for upscaling microfluidic emulsification devices

All of the above shows that the design of microfluidic emulsification devices are of utmost importance to improve overall productivity. DFU productivity can be increased by increasing flow resistance of the dispersed phase sub-structure. This will lead to a blow-up pressure that is substantially higher than the Laplace pressure of the empty interface. This pressure difference of such a device will always be positive, and droplets can be formed without the need for emulsifier adsorption taking place, which reduces down time and droplet formation time greatly. This will allow the DFU frequency to steeply increase (as shown in Fig. 2b for Partitioned EDGE). A similar effect may be achieved by increasing the surfactant concentration, since this will decrease the interfacial tension faster during down time, which increases the pressure difference.

If the DFUs do not get a sufficient supply of emulsifier, this will have two negative consequences: (1) coalescence may occur, which negatively impacts droplet monodispersity, and (2), droplet formation might not be taking place at downstream pores if SDS gets depleted; the interfacial tension of these menisci (Fig. 3d) will be close to the interfacial tension of a bare oil–water interface, which is higher than the blow-up pressure in the case of Multi EDGE, which could result in inactive DFUs. Therefore, we recommend to estimate how much emulsifier the droplet generator needs, which can be achieved by multiplying the formation frequency of droplets per DFU (58 s^{-1} for Multi EDGE) with the amount of active pores (70,000) the surface area of one droplet (3.8 E^{-10} m^2) and the interfacial load (~1 mg m^{-2}) (Berton-Carabin et al., 2014). So, for Multi EDGE that would be $1.5 \cdot 10^{-6}$ g/s. If an SDS concentration of 5 g/L is used, the lowest possible continuous phase flow rate to cover all droplets with SDS would be 1.1 mL per hour, and obviously, one would need to apply a flow rate of several times this amount for two reasons: (1) the droplets are formed at locations of low continuous phase flow, and it is undesirable to deplete the surfactant concentration there, and

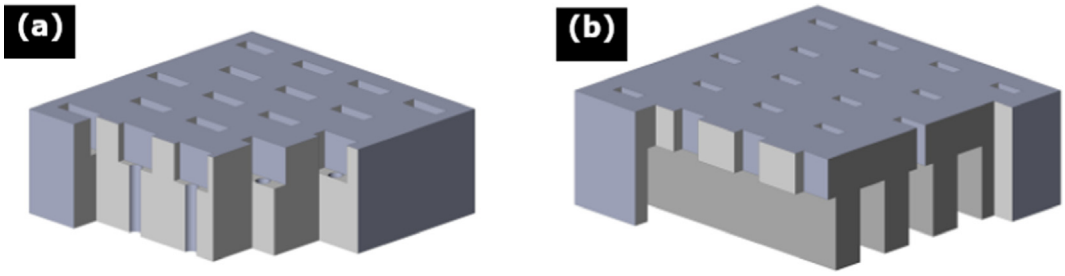

Fig. 4. Schematic 3D representation of asymmetric straight-through MCs (a), in comparison with Multi EDGE (b). Oil is pushed through the channels at the bottom and droplets form at the mouth of the slits on top.

(2), to decrease the interfacial tension faster during down time, which promotes droplet formation frequencies as explained above.

4. Conclusion

This work has shown that Multi EDGE devices enable stable production of 10-μm monodisperse hexadecane droplets at ~ 0.3 1 $m^3 \cdot m^{-2} \cdot h^{-1}$ over long periods of time, which brings the device close to industrially relevant values. We have shown that upscaled microfluidic emulsification devices should be designed wisely to further increase the productivity, which can be done by increasing the flow resistance of the dispersed phase sub-structure. The required pressure to reach maximum production (before blow-up occurs) is then higher, which leads to a larger driving force for refilling of the droplet formation unit, therewith effectively increasing the throughput. The down time can be minimized if the blow-up pressure is higher than the bare oil–water Laplace pressure of the meniscus in the droplet formation unit. If that is the case, surfactant adsorption is not required for refilling the droplet formation unit, which makes the refill fast. To make most out of the insights generated in this paper, current limitations in microfluidic chip design need to be mitigated, and we would like to challenge construction companies to help us make Multi EDGE a break-through technology.

Funding

This research was funded by the Dutch Research Council (NWO), Grant No 731.017.301.

Data availability

Data will be made available on request.

Declaration of Competing Interest

The authors declare that they have no known competing financial interests or personal relationships that could have appeared to influence the work reported in this paper.

Acknowledgements

We thank Maurice Strubel for his excellent technical assistance regarding the microfluidic set-up.

Appendix. On 'Upscaling microfluidic emulsification to industrially relevant throughputs: The importance of (sub-) structure design in EDGE devices'

Flow during necking and counter pressure

The flow during necking can be determined by recording the time the necking stage takes (t_{neck}) and the volume of the final droplet (V_{drop}):

$$\phi_{n,\ experimental} = \frac{V_{drop}}{t_{neck}} \tag{A1}$$

V_{drop} is determined as described in the main text and t_{neck} is determined by dividing the number of frames that the necking stage takes by the frame rate. The flow during necking was measured for Partitioned EDGE-10 at blow-up and compared with the theoretical flow during necking, which can be determined by the Hagen-Poiseuille equation:

$$\phi_{n,\ theory} = \frac{P_{app}}{R_{t,mi}} \tag{A2}$$

The results for $\phi_{n,\ theory}$ and $\phi_{n,\ experimental}$ differ only by 2 %, which suggests that there is no effective counter pressure during necking (Table A1).

Calculated blow-up pressure

The blow-up pressure has been argued to be the pressure at which the viscous forces from the dispersed phase flow start to dominate over the interfacial tension force in the neck (Dangla et al., 2013). Since differences in sub-structure of the EDGE devices are not expected to influence the interfacial tension force in the neck, we would expect that the flow during necking at blow-up would be the same for Partitioned EDGE-10 and Multi EDGE. Since the section above shows that there is not an effective counter pressure during necking, we can rewrite Equation A(2) to find the theoretical blow-up pressure of Multi EDGE, based on the maximum flow during necking for Partitioned EDGE($\phi_{n,\ experimental}$) and flow resistance calculated for one micro-plateau of Multi EDGE ($R_{t,mi}$):

$$P_{blow-up} = \phi_{n,\ experimental} \cdot R_{t,mi} \tag{A3}$$

When using the $\phi_{n,\ experimental}$ from Partitioned EDGE (Table A1) and the $R_{t,mi}$ from Multi EDGE (Table 3, main article), we find a theoretical blow-up pressure for Multi EDGE of 270 mbar. This is higher than the experimentally determined blow-up pressure of 130 mbar. As described in the main text, this could be due to a difference in contact angle of Multi EDGE and Partitioned EDGE or due to a different flow profile caused by the main plateau dimensions (especially the height).

References

Abrahamse, A.J., van Lierop, R., van der Sman, R.G.M., van der Padt, A., Boom, R.M., 2002. Analysis of droplet formation and interactions during cross-flow membrane emulsification. J. Memb. Sci. 204 (1-2), 125–137.

Amstad, E., Chemama, M., Eggersdorfer, M., Arriaga, L.R., Brenner, M.P., Weitz, D.A., 2016. Robust scalable high throughput production of monodisperse drops. Lab Chip 16 (21), 4163–4172.

Berton-Carabin, C.C., Ropers, M.-H., Genot, C., 2014. Lipid oxidation in oil-in-water emulsions: involvement of the interfacial layer. Compr. Rev. Food Sci. Food Saf. 13, 945–977. https://doi.org/10.1111/1541-4337.12097.

Charcosset, C., Limayem, I., Fessi, H., 2004. The membrane emulsification process—a review. J. Chem. Technol. Biotechnol. 79 (3), 209–218.

Conchouso, D., Castro, D., Khan, S.A., Foulds, I.G., 2014. Three-dimensional parallelization of microfluidic droplet generators for a litre per hour volume production of single emulsions. Lab Chip 14, 3011–3020.

Dangla, R., Fradet, E., Lopez, Y., Baroud, C.N., 2013. The physical mechanisms of step emulsification. J. Phys. D. Appl. Phys. 46 (11), 114003.

Deng, B., Schroën, K., de Ruiter, J., 2021. Effects of dynamic adsorption on bubble formation and coalescence in partitioned-EDGE devices. J. Colloid Interface Sci. 602, 316–324.

Eggersdorfer, M.L., Seybold, H., Ofner, A., Weitz, D.A., Studart, A.R., 2018. Wetting controls of droplet formation in step emulsification. Proc. Natl. Acad. Sci. 115 (38), 9479–9484.

Table A1
Results of flow during necking for Partitioned EDGE at blow-up.

Necking flow	V_{drop} (ml)	t_{neck} (ms)	P_{app} (Pa)	$R_{t,mi}$ (Pa s/m^3)	ϕ_n (ml/s)
Experimental	4.96×10^{-10}	0.335	–	–	1.48×10^{-6}
Theory	–	–	9.0×10^{4}	6.22×10^{16}	1.45×10^{-6}

Galvis, E., Yarusevych, S., Culham, J.R., 2012. Incompressible laminar developing flow in microchannels. J. Fluids Eng. 134, 14503.
Gijsbertsen-Abrahamse, A.J., van der Padt, A., Boom, R.M., 2004. Status of cross-flow membrane emulsification and outlook for industrial application. J. Memb. Sci. 230, 149–159 10.1016/j.memsci.2003.11.006.
Guo, X., Chen, M., Li, Y., Dai, T., Shuai, X., Chen, J., Liu, C., 2020. Modification of food macromolecules using dynamic high pressure microfluidization: A review. Trends Food Sci. Technol.
Kawakatsu, T., Kikuchi, Y., Nakajima, M., 1997. Regular-sized cell creation in microchannel emulsification by visual microprocessing method. J. Am. Oil Chem. Soc. 74, 317–321.
Kobayashi, I., Mukataka, S., Nakajima, M., 2004. Effect of slot aspect ratio on droplet formation from silicon straight-through microchannels. J. Colloid Interface Sci. 279, 277–280.
Kobayashi, I., Mukataka, S., Nakajima, M., 2005. Production of monodisperse oil-in-water emulsions using a large silicon straight-through microchannel plate. Ind. Eng. Chem. Res. 44, 5852–5856.
Kobayashi, I., Takano, T., Maeda, R., Wada, Y., Uemura, K., Nakajima, M., 2008. Straight-through microchannel devices for generating monodisperse emulsion droplets several microns in size. Microfluid. Nanofluidics 4, 167–177.
Kobayashi, I., Murayama, Y., Kuroiwa, T., Uemura, K., Nakajima, M., 2009. Production of monodisperse water-in-oil emulsions consisting of highly uniform droplets using asymmetric straight-through microchannel arrays. Microfluid. Nanofluidics 7, 107.
Kobayashi, I., Neves, M.A., Wada, Y., Uemura, K., Nakajima, M., 2012. Large microchannel emulsification device for mass producing uniformly sized droplets on a liter per hour scale. Green Process. Synth. 1, 353–362.
Maan, A.A., Sahin, S., Mujawar, L.H., Boom, R., Schroën, K., 2013. Effect of surface wettability on microfluidic EDGE emulsification. J. Colloid Interface Sci. 403, 157–159.
Montessori, A., Lauricella, M., Succi, S., Stolovicki, E., Weitz, D., 2018. Elucidating the mechanism of step emulsification. Phys. Rev. Fluids 3, 72202.
Montessori, A., Lauricella, M., Stolovicki, E., Weitz, D.A., Succi, S., 2019. Jetting to dripping transition: critical aspect ratio in step emulsifiers. Phys. Fluids 31, 21703.
Muijlwijk, K., Hinderink, E., Ershov, D., Berton-Carabin, C., Schroën, K., 2016. Interfacial tension measured at high expansion rates and within milliseconds using microfluidics. J. Colloid Interface Sci. 470, 71–79.
Neves, M.A., Wang, Z., Kobayashi, I., Nakajima, M., 2017. Assessment of oxidative stability in fish oil-in-water emulsions: effect of emulsification process, droplet size and storage temperature. J. Food Process Eng. 40, e12316.
Ofner, A., Moore, D.G., Rühs, P.A., Schwendimann, P., Eggersdorfer, M., Amstad, E., Weitz, D.A., Studart, A.R., 2017. High-Throughput Step Emulsification for the Production of Functional Materials Using a Glass Microfluidic Device. Macromol. Chem. Phys. 218.
Persson, K.H., Blute, I.A., Mira, I.C., Gustafsson, J., 2014. Creation of well-defined particle stabilized oil-in-water nanoemulsions. Colloids Surfaces A Physicochem. Eng. Asp. 459, 48–57.
Sahin, S., Bliznyuk, O., Cordova, A.R., Schroën, K., 2016. Microfluidic EDGE emulsification: the importance of interface interactions on droplet formation and pressure stability. Sci. Rep. 6, 26407.
Sahin, S., Schroën, K., 2015. Partitioned EDGE devices for high throughput production of monodisperse emulsion droplets with two distinct sizes. Lab Chip 15, 2486–2495.
Schroën, K., Bliznyuk, O., Muijlwijk, K., Sahin, S., Berton-Carabin, C.C., 2015. Microfluidic emulsification devices: from micrometer insights to large-scale food emulsion production. Curr. Opin. Food Sci. 3, 33–40.
Shen, B., Ricouvier, J., Malloggi, F., Tabeling, P., 2016. Designing colloidal molecules with microfluidics. Adv. Sci. 3.
Stolovicki, E., Ziblat, R., Weitz, D.A., 2018. Throughput enhancement of parallel step emulsifier devices by shear-free and efficient nozzle clearance. Lab Chip 18, 132–138.
Ten Klooster, S., Sahin, S., Schroën, K., 2019. Monodisperse droplet formation by spontaneous and interaction based mechanisms in partitioned EDGE microfluidic device. Sci. Rep. 9, 1–12.
Theberge, A.B., Courtois, F., Schaerli, Y., Fischlechner, M., Abell, C., Hollfelder, F., Huck, W.T.S., 2010. Microdroplets in microfluidics: an evolving platform for discoveries in chemistry and biology. Angew. Chemie Int. Ed. 49, 5846–5868.
van Dijke, K., Veldhuis, G., Schroën, K., Boom, R., 2009. Parallelized edge-based droplet generation (EDGE) devices. Lab Chip 9, 2824–2830.
van Dijke, K., de Ruiter, R., Schroën, K., Boom, R., 2010a. The mechanism of droplet formation in microfluidic EDGE systems. Soft Matter 6, 321–330.
van Dijke, K., Kobayashi, I., Schroën, K., Uemura, K., Nakajima, M., Boom, R., 2010b. Effect of viscosities of dispersed and continuous phases in microchannel oil-in-water emulsification. Microfluid. Nanofluidics 9, 77–85.
Van Dijke, K.C., Schroën, K.C., Boom, R.M., 2008. Microchannel emulsification: from computational fluid dynamics to predictive analytical model. Langmuir 24, 10107–10115.
van Dijke, K.C., Schroën, K., van der Padt, A., Boom, R., 2010c. EDGE emulsification for food-grade dispersions. J. Food Eng. 97, 348–354.
van Dijke, K.C., Veldhuis, G., Schroën, K., Boom, R.M., 2010d. Simultaneous formation of many droplets in a single microfluidic droplet formation unit. AIChE J. 56, 833–836.
Vladisavljević, G.T., Kobayashi, I., Nakajima, M., 2011. Effect of dispersed phase viscosity on maximum droplet generation frequency in microchannel emulsification using asymmetric straight-through channels. Microfluid. Nanofluidics 10, 1199–1209.
Vladisavljević, G.T., Kobayashi, I., Nakajima, M., 2012. Production of uniform droplets using membrane, microchannel and microfluidic emulsification devices. Microfluid. Nanofluidics 13, 151–178.
Vladisavljević, G.T., Ekanem, E.E., Zhang, Z., Khalid, N., Kobayashi, I., Nakajima, M., 2018. Long-term stability of droplet production by microchannel (step) emulsification in microfluidic silicon chips with large number of terraced microchannels. Chem. Eng. J. 333, 380–391 10.1016/j.cej.2017.09.141.
Zhu, P., Wang, L., 2017. Passive and active droplet generation with microfluidics: a review. Lab Chip 17, 34–75.